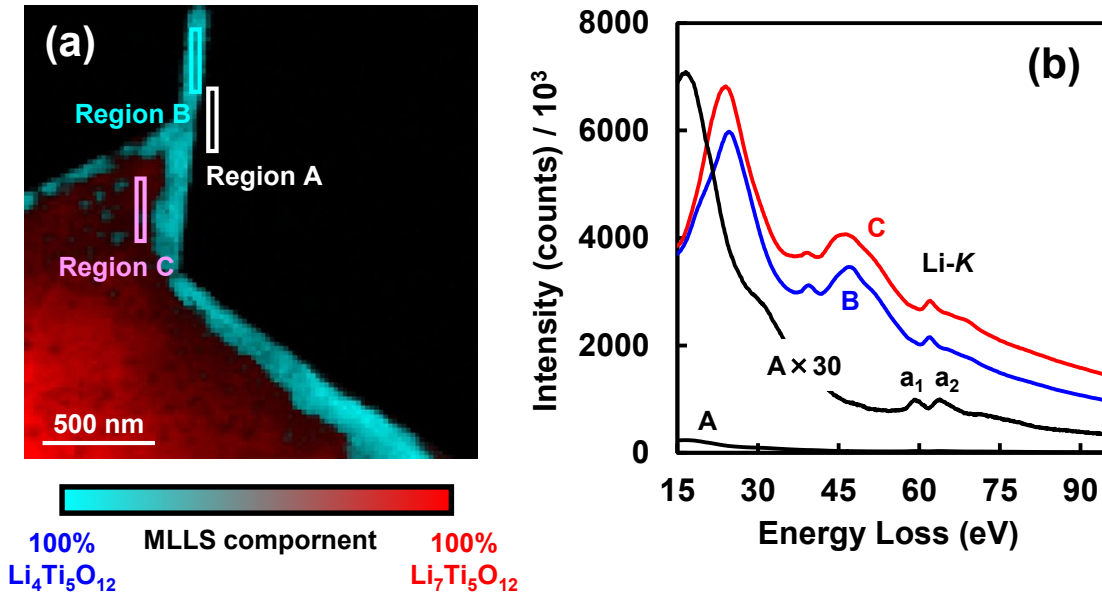


Supporting Information of  
Nanoscale-controlled Li-insertion reaction induced  
by scanning electron-beam irradiation in a  $\text{Li}_4\text{Ti}_5\text{O}_{12}$   
electrode material for lithium-ion batteries.

*Mitsunori Kitta\* and Masanori Kohyama*

Research Institute of Electrochemical Energy, National Institute of Advanced Industrial Science  
and Technology (AIST), 1-8-31, Midorigaoka, Ikeda, Osaka 563-8577, Japan



**Figure S1.**

EELS spectrum image of the electrochemically lithiated specimen stored in air for about 10 minutes. (a) MLLS deconvolution mapping image of Ti-L edge region (456-473 eV).  $\text{Li}_7\text{Ti}_5\text{O}_{12}$  and  $\text{Li}_4\text{Ti}_5\text{O}_{12}$  phases are indicated by red and blue colors, respectively. The  $\text{Li}_4\text{Ti}_5\text{O}_{12}$  phase is concentrated on the edge region of the specimen, which means the Li extraction (oxidation) reaction progressed from the surface of the lithiated specimen. Gas molecules in air (mainly oxygen) should concern the oxidation reaction. (b) EELS spectra of low-loss regions extracted from the regions (A), (B) and (C) on the image (a). The Li-K edge features of (B) and (C) are in good agreement with those of the  $\text{Li}_4\text{Ti}_5\text{O}_{12}$  and  $\text{Li}_7\text{Ti}_5\text{O}_{12}$  phases, respectively. The spectrum (A) extracted from the surface region of the specimen is also shown, while the intensity is 1/30 of the spectrum (B) or (C). The feature of Li-K edge of (A) is greatly different from that in (B) or (C). There are clear two peaks of  $a_1$  (59.1 eV) and  $a_2$  (63.8 eV), which agrees with the spectrum feature of  $\text{Li}_2\text{O}$ , discussed in EELS,<sup>S1,S2</sup> and soft-X-ray absorption spectrometry.<sup>S3</sup> Therefore, we can regard the surface product as  $\text{Li}_2\text{O}$ . Unit volumes of  $\text{Li}_2\text{O}$  and  $\text{Li}_7\text{Ti}_5\text{O}_{12}$  are  $14.9 \text{ cm}^3 / \text{mol}$  and

132 cm<sup>3</sup> / mol, respectively, and about 8.5 nm thick of Li<sub>2</sub>O was estimated. The thickness of the Li<sub>2</sub>O layer should be less than 1/10 of the wafer, resulting in a very weak EELS signal from Li<sub>2</sub>O.

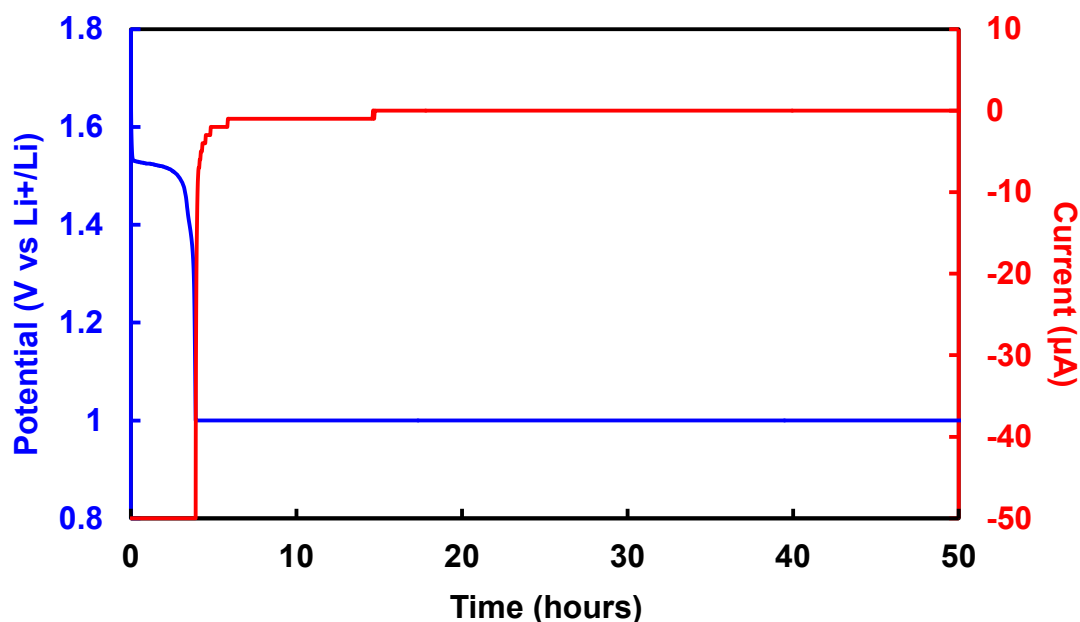


**Figure S2.**

Electrochemical Li-insertion process of a  $\text{Li}_4\text{Ti}_5\text{O}_{12}$  (LTO) electrode specimen to form a  $\text{Li}_7\text{Ti}_5\text{O}_{12}$  (Li-LTO) specimen. Commercial LTO powder (LT-106, Ishihara Sangyo Kaisha) of about 1.3 mg was loaded on a Cu mesh film and pressed into a sheet, which was used as a positive electrode in an electrochemical cell, assembled in dry-air ( $-80^\circ\text{C}$  d. p.) filled box with a Li-metal negative electrode and a liquid electrolyte (1 M  $\text{LiPF}_6$  in EC/DMC = 1). Electrochemical test was performed galvanostatically from open circuit potential to 1.0 V vs  $\text{Li}^+/\text{Li}$  with 50  $\mu\text{A}$  of constant cell current. Then the cell was stored at 1.0 V vs  $\text{Li}^+/\text{Li}$  with potentiostatic condition for 50 hours so as to complete the Li insertion. Voltage and current profiles of this electrochemical process are shown in figure S2 by blue and red solid lines, respectively. After the Li insertion, the LT-106 electrode was washed by DMC-solvent with ultrasonic bath for transmission electron microscopy analysis.

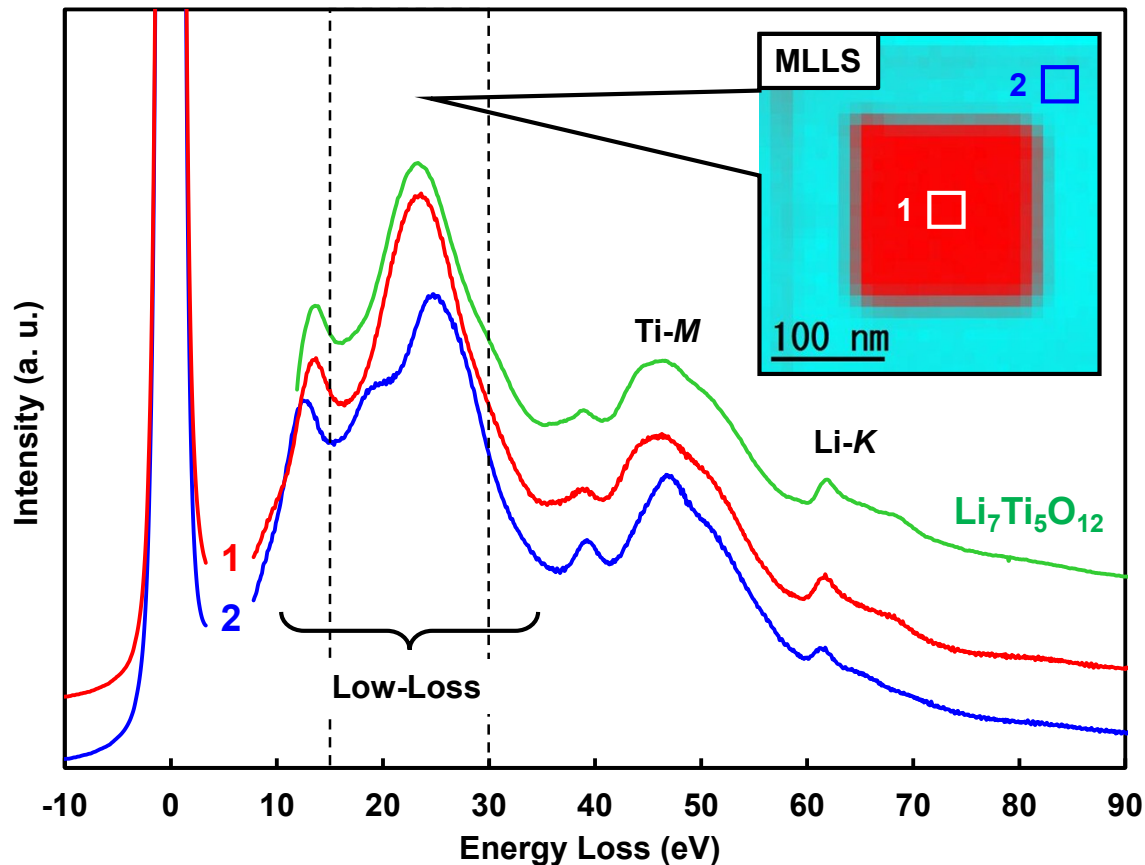


**Figure S3.**

Low-loss spectra of the specimen as presented in Fig. 1(b). Li-K edge and Ti-M edge peaks are observed at around 60 eV and 47 eV, respectively. The Li-K edge intensity in spectrum 1 is higher than that in spectrum 2, indicating the Li-insertion reaction at the high-dose irradiation area. The shape of Ti-M edge is also different in these two spectra, and the peak broadening can be seen in spectrum 1, similar to the  $\text{Li}_7\text{Ti}_5\text{O}_{12}$  spectrum. This feature would be derived from the reduction of Ti ions as  $\text{Ti}^{4+} \rightarrow \text{Ti}^{3+}$  by the Li-insertion. The spectra below 40 eV as a low-loss region include many energy-loss factors, such as phonon excitations, interband and intraband transitions, plasmon excitations, and so on. Therefore the spectra of this region is highly complicated and difficult to be assigned clearly. However, there are also clear differences between spectra 1 and 2 in this region, which seems to be caused by the different oxidation state of Ti. The reduction of  $\text{Ti}^{4+}$  is

accompanied by the change of electron conductivity and optical properties ( $\text{Li}_4\text{Ti}_5\text{O}_{12}$  is white and  $\text{Li}_7\text{Ti}_5\text{O}_{12}$  is almost black), which means the change in dielectric properties, affecting the low-loss spectrum. This spectrum change is useful as a fingerprint to distinguish the two phases. As an example, we performed MLLS deconvolution with 15-30 eV regions of spectra 1 and 2 indicated by two broken lines. As shown in the inset, the two-phase distribution similar to Fig. 2(a) can be well reproduced.

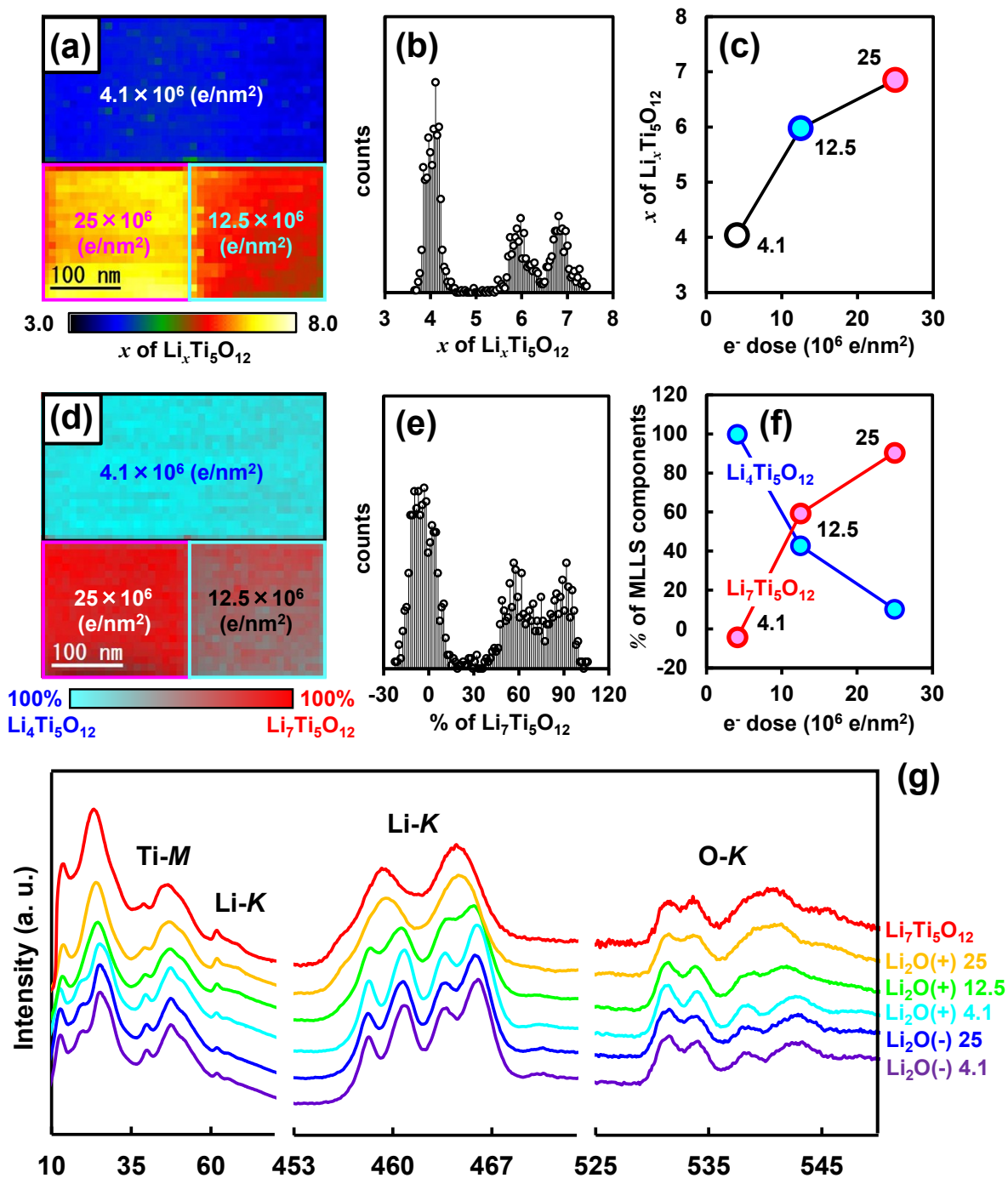


Figure S4

Investigation of the relation between the reaction progress and the electron-dose amount. (a) Li-K intensity map for the areas of three kinds of dose amounts. Each pixel grid values of Li-K intensity were normalized with  $x = 4$  for  $\text{Li}_4\text{Ti}_5\text{O}_{12}$ . The irradiation dose amounts were  $4.1 \times 10^6$

(electrons/nm<sup>2</sup>),  $12.5 \times 10^6$  (electrons/nm<sup>2</sup>) and  $25.0 \times 10^6$  (electrons/nm<sup>2</sup>) for the areas surrounded by black, cyan and magenta solid lines, respectively. The Li-*K* edge intensity was clearly increased with the electron-dose amount. (b) Histogram of the Li-*K* edge intensity analyzed from the whole area of (a). Three peaks with different Li compositions are observed clearly, and each peak corresponds to each area of the different dose amount in (a). (c) Relation between the Li composition and the electron-dose amount, derived from the histogram data in (b). The vertical value *x* was decided by the peak median position in (b). The Li composition is clearly increased with the electron-dose amount, while the increment is restricted by the Li<sub>7</sub>Ti<sub>5</sub>O<sub>12</sub> phase (*x* = 7). (d) The MLLS deconvolution image of Li<sub>4</sub>Ti<sub>5</sub>O<sub>12</sub> and Li<sub>7</sub>Ti<sub>5</sub>O<sub>12</sub> phases by using the Ti-*L* edge spectra for the same whole area of (a). The two areas of the minimum and maximum composites of Li<sub>7</sub>Ti<sub>5</sub>O<sub>12</sub> naturally correspond to the areas of the lowest and highest Li compositions in (a), respectively, according to the minimum and maximum dose amounts for the two areas. In the area of the middle electron-dose amount,  $12.5 \times 10^6$  (electrons/nm<sup>2</sup>), it seems that the two phases are overlapped along the electron beam direction. In other words, the Li<sub>7</sub>Ti<sub>5</sub>O<sub>12</sub> phase growth in a Li<sub>4</sub>Ti<sub>5</sub>O<sub>12</sub> thin crystal is stopped in the middle. This feature is clearly observed in the histogram of the composite ratio (MLLS component) from the whole area of (d) as shown in (e). The ratio of the Li<sub>7</sub>Ti<sub>5</sub>O<sub>12</sub> phase (%) shows three peaks, indicating that the depth of Li<sub>7</sub>Ti<sub>5</sub>O<sub>12</sub> phase generation is different for the three areas with different electron-dose amounts. (f) Relation between the ratio of the generated Li<sub>7</sub>Ti<sub>5</sub>O<sub>12</sub> phase and the electron-dose amount. The vertical value % was decided by the peak median position in the histogram of (e). For the plots in (c) and (f), we can see approximately-proportional relation between the electron-dose amount and the amount of the generated Li<sub>7</sub>Ti<sub>5</sub>O<sub>12</sub> phase. Of course, the total amount of the Li<sub>7</sub>Ti<sub>5</sub>O<sub>12</sub> phase is restricted by the initial amount of Li<sub>2</sub>O on the Li<sub>4</sub>Ti<sub>5</sub>O<sub>12</sub> surface, and the Li<sub>7</sub>Ti<sub>5</sub>O<sub>12</sub> phase is the final product by the

present beam-assisted Li insertion, instead of  $\text{Li}_9\text{Ti}_5\text{O}_{12}$  or more Li-insertion phases, due to the thermodynamic stability.<sup>S4,S5</sup> Therefore, much higher dose amounts, exceeding the  $\text{Li}_2\text{O}$  amount, may lead to the deterioration of the generated  $\text{Li}_7\text{Ti}_5\text{O}_{12}$  phase. (g) EELS spectra of  $\text{Li}_4\text{Ti}_5\text{O}_{12}$  specimens with and without  $\text{Li}_2\text{O}$  layers, indicated by  $\text{Li}_2\text{O}(+)$  and  $\text{Li}_2\text{O}(-)$ , respectively, after the electron-beam irradiation of three kinds of dose amounts,  $4.1 \times 10^6$ ,  $12.5 \times 10^6$  and  $25.0 \times 10^6$  (electrons/ $\text{nm}^2$ ). For  $\text{Li}_2\text{O}(-)$ , there are no spectrum changes, namely no Li-insertion reaction, even by the highest dose ( $25.0 \times 10^6$ ). For  $\text{Li}_2\text{O}(+)$ , the higher two dose amounts can induce the spectrum changes, while the complete change similar to the  $\text{Li}_7\text{Ti}_5\text{O}_{12}$  spectrum requires the highest dose ( $25.0 \times 10^6$ ).

## REFERENCES

- S1 X. H. Liu, J. W. Wang, Y. Liu, H. Zheng, A. Kushima, S. Huang, T. Zhu, S. X. Mao, J. Li, S. Zhang, W. Lu, J. M. Tour, J. Y. Huang, *Carbon*, 2012, **50**, 3836-3844.
- S2 N. Jiang, J. C. H. Spence, *Phys. Rev. B*, 2004, **69**, 115112.
- S3 R. Qiao, Y.-D. Chuang, S. Yan, W. Yang, *Plos One*, 2012, **7**, e49182.
- S4 T.-F. Yi, S.-Y. Yanga, Y. Xie, *J. Mater. Chem. A*, 2015, **3**, 5750-5777.
- S5 T.-F. Yi, H. Liu, Y.-R. Zhu, L.-J. Jiang, Y. Xie, R.-S. Zhu, *J. Power Sources*, 2012, **215**, 258-265.